ABSTRACT

This paper describes the behaviour of restrained steel columns in fire. It follows the introduction of extra load into the column through the axial restraint of the surrounding cooler structure and the consequential buckling. Key to this understanding is the post-failure behaviour and re-stabilisation of the column, which is discussed with reference to a finite element model and an analytical model. Through bi-directional control of the temperature, the finite element model allows the snap-back behaviour to be modelled in detail and the effects of varying slenderness and load ratio are investigated. The analytical model employs structural mechanics to describe the behaviour of a heated strut, and is capable of explaining both elastic and fully-plastic post-buckling behaviour.

Through this detailed explanation of what happens when a heated column buckles, the consequences for steel framed building design are discussed. In particular, the need to provide robustness is highlighted, in order to ensure alternative load-paths are available once a column has buckled and re-stabilised. Without this robustness, the dynamic shedding of load onto surrounding structures may well spread failure from a fire's origin and lead to progressive collapse.

Keywords: Steel, Columns, Buckling, Fire resistance, Axial Forces, Nonlinear analysis

NOTATION

E	Elastic (Young's) modulus
A	Member cross-sectional area
l	Member length
I	Member second moment of area
P	External force at column top
F	Internal force in column
$F_E = \pi^2 EI / l^2$	Column Euler buckling force at ambient temperature
K	Restraint stiffness at column top
K_b	Beam Flexural bending stiffness
$K_c = EA / l$	Column axial stiffness
K_{ET}	Elastic modulus reduction with temperature factor
K_{yT}	Yield strength reduction with temperature factor
M_p	Plastic moment capacity of column (assumed invariant with axial force)
$\rho = K / K_c$	Restraint ratio
$\overline{\rho} = Kl / F_E$	Restraint ratio (normalised with respect to the Euler buckling force)
δ	Axial deflection of the top of the strut
$\overline{\delta} = \delta / l$	Normalised axial deflection of the top of the strut
Δ	Lateral deflection of the mid-height of the strut
$\overline{\Delta} = \Delta / l$	Normalised lateral deflection of the mid-height of the strut
λ	Column slenderness ratio
$\mu = P / F_E$	External load ratio (normalised with respect to the Euler buckling force)
$\overline{\mu} = P / EA$	External load ratio (normalised with respect to axial stiffness)
$\phi = F / F_E$	Internal load ratio (normalised with respect to the Euler buckling force)
$\gamma = M_p / (\pi^2 EI / l)$	Plastic moment of column (normalised with respect to Euler x length)

INTRODUCTION

1.1 Context

As the full-scale fire tests at Cardington have shown [1], whilst the majority of beams in a steel-framed building can be designed to function without the need for fire protection, columns are so critical to the load carrying capacity of a building that they must remain protected. A failure of a column on one floor can have a great effect on the floors above, meaning fire compartments can be breached and there is a danger of disproportionate collapse.

It is also the case that all columns in building frames are subject to axial restraint, since their purpose is to support structure above and this structure will have a vertical stiffness. It is therefore hugely important that the behaviour of columns in fire is understood, and in particular, the role that axial restraint plays in this behaviour.

A number of researchers have looked at this role, from both an experimental and analytical point of view. For example Ali *et al.* [2], Rodrigues *et al.* [3] and Tan *et al.* [4] have all performed physical experiments on axially restrained columns at elevated temperatures. Shepherd *et al.* [5], Franssen [6] and Huang & Tan [7] have simulated such tests using finite element analysis techniques and extended these simulations to further investigate the role of axial restraint.

In this paper, the theoretical explanation behind the behaviour of steel columns in fire is presented, alongside the results of finite element analyses in order to illustrate particular characteristics of this explanation. Specifically, the differences in behaviour of columns pre- and post-buckling are contrasted and the details of snap-back buckling examined.

1.2 Modelling

The behaviour of columns outlined in this paper is demonstrated through finite element analysis using a simplified model of an axially restrained column (see Figure 1). All test cases model a 203x203x52UC pin-ended column of Grade 43 steel and length 5.16m to give a minor-axis slenderness of 100. The column was divided into eight finite elements along its length and given an initial geometric imperfection and load ratio of 0.6 according to EC3 design rules. The finite element analysis was performed using the Vulcan program (http://www.vulcan-solutions.com/, accessed Feb 2010), which incorporates geometric non-linearities and uses EC3 Part 1-2 material property variation to define how the elastic modulus and yield strength deteriorate with temperature.

Axial restraint was provided by an axial spring element at the same end of the column as the applied load. This elastic restraint was quantified by the use of the Relative Restraint Ratio, which is the ratio of the axial stiffness of the restraint to the ambient-temperature axial stiffness of the heated column, as defined by Wang and Moore [8]. All columns were uniformly heated, both in cross-section and along their length, thus eliminating the effect of time-temperature history in generating spatial temperature distributions. All analyses are controlled by stepping up or down in temperature, so that time effects are not incorporated and no particular time-based fire-curve need be considered.

All forces reported are the axial forces in the column element at the top of the column and any displacements refer to the axial displacement of the top of the column, measured from the initial unloaded datum position.

2 LOADING

2.1 Explanation

When a steel column is heated it thermally expands. If this column is part of a building frame, it will exert an upwards force on the ends of any beams framing in to its top and any columns directly above. Firstly let us consider the single-storey (or top-storey) case where there are no columns above.

If the columns at the other ends of the beams which frame-in (i.e. one bay away) remain cool (see Figure 2a), the beams will undergo differential vertical movement of their ends, inducing flexure and they will therefore exert a restraining force on the heated column in question, resisting its vertical expansion. If however the surrounding columns are also heated at a similar rate (i.e. they are within the same fire-compartment) (see Figure 2b) then both ends of the beams will undergo the same vertical movement and no restraining force will be introduced. There will of course generally be a restraining force on the surrounding columns. Only when an entire floor is heated at exactly the same rate (see Figure 2c) will all the columns escape the addition of a restraint force, since they will all thermally expand together and no relative vertical movement will be present to cause flexure in the connecting beams.

If the presence of an upper-floor is also taken into account, the situation is similar. But force due to the thermal expansion of the column (or group of columns) is also passed up through the columns of the floor above (see Figure 3) into the beams above. Since the columns above have an axial stiffness, only a proportion of the movement reaches the beams above, but once it does, this movement is resisted through flexure in exactly the same way as the beams below.

Simple mathematical models exist [9, 10] which can be used to calculate the level of axial restraint likely to be experienced by a column, and can take into account effects of beams, columns, composite floors, upper storeys, rotational restraint, etc. This allows a complex frame arrangement to be analysed using a simplified finite element model, with a single spring element representing the axial restraint applied to the column.

In the case of a single storey, the restraint stiffness experienced by a heated column, K_r, is simply the sum of the vertical stiffnesses of the beams which frame in to the top. For example, the two-dimensional case shown in Figure 2a has a restraining stiffness given by Equation 1.

$$K_r = \sum_{i=1}^{\substack{number\ of\\ restraining\\ beams}} K_{bi} = K_{b1} + K_{b2} \qquad (1)$$

For example, the stiffness of the heated 254x254x167UC column shown in Figure 4, K_c, can be found from Equation 2

$$K_c = \frac{EA}{L} = \frac{210{,}000\ x\ 21{,}300}{3600} = 1{,}242{,}500\ N/mm \tag{2}$$

The stiffness experienced by the heated column from each lower floor 305x165x54UB restraining beam, K_{b1}, can be calculated as Equation 3

$$K_{b1} = \frac{12EI}{L^3} = \frac{12\ x\ 210000\ x\ 116960000}{6000^3} = 1365\ N/mm \tag{3}$$

And the stiffness, K_{b2}, from each upper floor beam when the largest, 914x419x388UB section is present can be calculated as Equation 4

$$K_{b2} = \frac{12EI}{L^3} = \frac{12\ x\ 210000\ x\ 7196350000}{6000^3} = 83957\ N/mm \tag{4}$$

A simplified calculation can therefore be performed, which ignores the stiffness of the second floor column; this was used by Bailey and Newman [11] to calculate the relative restraint ratio for the heated column in Figure 4 subject to two of each beam-type, as Equation 5

$$\rho = \frac{2K_{b1} + 2K_{b2}}{K_c} = \frac{2\times 1365 + 2\times 83957}{1242500} = 0.138 \tag{5}$$

However, for a two-storey structure as shown in Figure 3, the restraint experienced by a heated ground-floor column should also include the axial stiffness of the second floor column, as well as the stiffness of the restraining beams on each floor above. In this case the stiffness of the upper column and the second-floor beams are combined in series, as shown in Equation 6.

$$K_r = K_{floor1} + \frac{1}{\frac{1}{K_{column2}} + \frac{1}{K_{floor2}}} = 2K_{b1} + \frac{1}{\frac{1}{K_{c2}} + \frac{1}{2K_{b2}}} \tag{6}$$

As shown with dotted lines in Figure 3, this system can be extended to any number of floors above the heated column by generating more deeply nested continued fractions.

In the common case where a frame consists of a single section size for all the columns and another for all the beams, an upper bound can be established for the restraint stiffness by calculating the restraint that would be theoretically applied if there were infinitely many upper storeys. If K_b represents the vertical restraining stiffness of all the beams on a single floor that frame in to a column-top, and K_c represents the axial stiffness of each column, then the restraint provided by infinite floors, K_∞ would be as shown in Equation 7 below.

$$K_\infty = K_b + \cfrac{1}{\cfrac{1}{K_c} + \cfrac{1}{K_b + \cfrac{1}{\cfrac{1}{K_c} + \cfrac{1}{K_b + \cfrac{1}{\cfrac{1}{K_c} + \cfrac{1}{K_b + \cfrac{1}{\cfrac{1}{K_c} + \ddots}}}}}}}} \tag{7}$$

Since this is an infinite continued fraction, the fraction K_∞ can be substituted in to itself, as shown in the first part of Equation 8.

$$K_\infty = K_b + \frac{1}{\frac{1}{K_c} + \frac{1}{K_\infty}} = K_b + \frac{K_\infty}{\frac{K_\infty}{K_c} + 1} = \frac{K_b\left(\frac{K_\infty}{K_c} + 1\right) + K_\infty}{\frac{K_\infty}{K_c} + 1} \tag{8}$$

And this can be solved for K_∞ as follows in Equations. 9-11:

$$\Rightarrow K_\infty\left(\frac{K_\infty}{K_c} + 1\right) = K_b\left(\frac{K_\infty}{K_c} + 1\right) + K_\infty \tag{9}$$

$$\Rightarrow \frac{{K_\infty}^2}{K_c} + K_\infty = \frac{K_b K_\infty}{K_c} + K_b + K_\infty \tag{10}$$

$$\Rightarrow {K_\infty}^2 - K_b K_\infty - K_b K_c = 0 \tag{11}$$

Equation 11 is quadratic in K_∞ and can therefore be solved in the usual way as shown in Equation 12.

$$K_\infty = \frac{K_b \pm \sqrt{{K_b}^2 + 4K_b K_c}}{2} \tag{12}$$

Since the stiffness values K_b and K_c are both positive, the quantity inside the square-root is > ${K_b}^2$, and therefore the only solution which makes physical sense (i.e. gives a positive value for K_∞) is when the positive square-root is used, giving Equation 13.

$$K_\infty = \frac{K_b + \sqrt{{K_b}^2 + 4K_b K_c}}{2} \tag{13}$$

This value is the restraint experienced by a column with an infinite number of identical floors above it, it is an upper-bound on the axial restraint provided to the ground floor column, and for that matter any column within the frame.

2.2 Modelling

The test column was analysed with a range of restraint spring stiffness to model the effects of Restraint Factors ranging from the very low (0.004) to the very high (0.138). These values do not necessarily aim to model realistic values of restraint seen in building frames, which are usually in the range of 0.02-0.03 [8], but more to show the difference in behaviour from columns with very low and very high restraint levels. They are based on previous work by Bailey and Newman [11] which takes a simple 2D two-storey frame as a base model and changes the section size of the top beam to vary the restraint applied to the column as shown in Figure 4.

The axial force present in the columns, due to the combination of the externally imposed load and restrained thermal expansion, is shown in Figure 5 for the pre-buckling heating phase. The initial part of the curves (at ambient 20°C) shows that higher the axial restraint results in a lower force in the column. This is to be expected, since the slack axial springs are introduced before loading has been applied, and the higher level of axial restraint is provided by a stiffer axial spring, which will attract a greater proportion of the applied load as it is applied. A less-stiff restraint spring will shed more of the applied load onto the column itself.

The main feature of the graph is clearly that the columns with higher restraint increase their force quicker than the less-restrained columns. This is obvious from the fact that the increase in temperature results in a thermal strain, which is directly converted into a stress (and therefore force) through the stiffness of the restraint.

Another, less obvious feature is that all the curves pass through a single point around 50°C when the thermal expansion has overcome the initial shortening due to applied load. Even though the highly restrained columns began with less force, this force increases quicker with temperature until they reach the exact same value of force as the less restrained columns. The explanation of this becomes clear when it is noted that at this point the thermal strain has exactly overcome the shortening due to loading, therefore the restraint spring is exactly back to its original unstressed length. The spring has therefore not been mobilised, and may as well not even be present. Its stiffness must therefore be irrelevant and each test case with a different spring must reach this point at the same temperature.

3 BUCKLING

3.1 Explanation

As heating progresses, the force in the column continues to increase until the buckling load of the column is reached. Although the column sections are all the same, and therefore their ambient buckling loads would be identical, this load is achieved at different temperatures, depending on how quickly the restraint force is increasing. Since the highly restrained columns gain restraint force quickly, they reach the buckling load sooner (i.e. at a lower temperature) and since at this lower temperature the material properties (stiffness and yield stress) have not degraded much, the buckling load is relatively high and a high level of column force can be achieved. The lower restrained columns don't reach their buckling load until they are much hotter, but at this stage the material properties have

degraded sufficiently to result in a much lower value of buckling load. As the temperature rises, at the same time as the restraint force is increasing due to axial restraint, the buckling load is decreasing due to material properties changing, and at some point these to come together to initiate a buckling failure in the column.

When buckling occurs, the analysis shows the columns undergo a sudden shortening and become shorted than their original length. This results in a shedding of load back onto the restraint spring and the force in the column is seen to suddenly reduce. Since the analysis steps up in small temperature increments, this exhibits itself by what seems like snap-through behaviour. Figure 6 describes this behaviour in the Displacement-Temperature domain where curve “a” shows the increase in displacement due to thermal expansion against the axial restraint and curve “b” shown this sudden snap-through and if heating is continued, the column would follow curve “c”. Most existing experimental studies [6, 12] have exhibited this type of sudden buckling behaviour because, during a real fire test, it is impossible to predict exactly when a column might fail and then adjust the heating regime sufficiently to control the behaviour of the column during buckling.

3.2 Modelling

For a given level of restraint, an initial analysis was performed to assess the behaviour of the columns up-to and beyond buckling. The results in the force domain are shown on Figure 7 and similar behaviour to the deflection curves “a”, “b” and “c” of Figure 6 can be seen. After buckling, the columns re-stabilise in a state where their shortening by buckling is more than their lengthening through thermal expansion and they are overall shorter than their original length. In this state they are essentially hanging from their restraint springs and carry little axial force. As the temperature continues to increase their force decreases in line with their reduction in stiffness as they shed more and more load onto the restraint spring. The little extra thermal expansion they undergo, which would tend to increase their axial force as they pick up load from the restraint is negligible compared to the more dominant reduction in stiffness. The kink in the curves of Figure 7 at 400°C directly reflects the change in material properties that occurs at this same temperature in the Eurocodes and also therefore Vulcan. By 1200°C hardly any strength remains in the columns themselves and the force tails off towards zero.

The analyses of the four columns with least axial restraint are not able to find numerical post-buckling solutions due to huge numerical instability associated with this jump from one stable solution to another. Since the restraint stiffness is much lower, the overall stiffness present in the system is also lower, the global stiffness matrix therefore becomes ill-formed and the solution procedure fails to converge.

4 SNAP-BACK

4.1 Explanation

Most existing experimental studies [6, 12] have exhibited the type of sudden snap-through buckling behaviour outlined above since it is impossible to control the behaviour of the column during buckling.

With an analytical model however, full control over the temperature parameters is available at every stage and the analysis is exactly repeatable, allowing this buckling to be studied in more detail.

In particular the effect of *reducing* the temperature of the columns after buckling can be investigated. As the temperature is reduced, the force in the column increases, since the material properties of the column are restored. This leads to the column stiffness increasing, thereby taking a greater proportion of the load from the restraint spring. This is represented as curve “d” in Figure 6 and continues until there no longer exists this post-buckled solution. If the temperature is lowered even further, the solution would snap-up along curve “e” to the initial loading solution, whereby it would continue to unload along curve “f” back to ambient temperature. This initial loading solution is stable and therefore if the model were to be heated once again at this stage, it would continue up the loading path along curve “g” once again.

It can be seen that in the temperature range from curve “e” to “b” in Figure 6 there exist two stable solutions, one pre-buckled and the other post-buckled, in which the column can be in equilibrium By putting the current state of the finite element analysis into one of the regions where only one stable state exists (either lower temperatures than curve “e” or higher than curve “b”) the analysis can be forced into one or other of the two states, and this state can be followed up or down in temperature. It can be inferred that the “numerical” solution path of a heated column would be the path “a”-“h”-“d”-“c” in Figure 6 if only it were possible to observe it directly.

4.2 Modelling

For those analyses where stable post-buckled solutions had been found, each was repeated up the buckling temperature of each column (the bottom point of curve “b” in Figure 6) and then the temperature was reduced to follow curve “d” back through equilibrium points not measurable during physical tests. Eventually the analyses “snapped-up” and began to go back down the original loading path. The results of these cooling phases have then been incorporated into those of the heating analyses by reversing the results from the curve “d” parts of the analyses and inserting them between the top and bottom of the curve “b” parts of the analyses. The resulting trace of equilibrium positions in the force domain is shown in Figure 8.

The corresponding displacement domain results are shown in Figure 9 for completeness. It can be seen from Figure 9 that at 1200°C, when there is very little strength left in the column itself, the vertical displacement of the top of the column is wholly dependent on the stiffness of the restraint spring that carries the applied load. It can also be seen that there exists a second point around 180°C where all the curves pass through a single point. This again represents the point at which the column becomes equal to its original length and therefore the spring is not active and its stiffness is irrelevant. This is an exact parallel of what happened during loading, but is slightly less well defined on the graph since results either side of buckling are interpolated with straight lines through this point.

5 SIMPLE RATIONALISATION

The snap-through behaviour seen in the finite element results is not necessarily intuitively understandable, and it is therefore worthwhile to use normal structural mechanics to attempt to model the behaviour of a heated column, axially loaded in compression at its top and under the influence of elastic axial restraint to thermal expansion. Consider a perfectly straight simple elasto-plastic steel strut of length l and cross-sectional area A, shown in Figure 10(a), pinned to allow free rotation at its top and bottom and restrained against axial movement at its top by an elastic spring of stiffness K which is a proportion ρ of the axial stiffness of the strut at 20°C, so $K = \rho K_c$.

The steel of the strut has a constant coefficient of thermal expansion α, so as its temperature is raised from 20°C to T°C its "natural" length increases to $l(1+\alpha(T-20))$. It is assumed that the elastic modulus of the strut's steel reduces with temperature as shown in Figure 11(a), following the reduction factor k_{ET}, in a smoother fashion than if it were in accordance with the assumption of EN1993-1-2. For the purposes of this illustrative example the degradation of elastic modulus with temperature is expressed as

$$k_{ET} = 1.0 \qquad (T \le 100\,°C)$$

$$k_{ET} = -2.667 + 9373.4/(T + 2456.0) \qquad (T > 100\,°C)$$

The yield strength is assumed to decline, again in a smoother fashion than EN1993-1-2 demands, as shown in Figure 11(b):

$$k_{yT} = 1.0 \qquad (T \le 400\,°C)$$

$$k_{yT} = -0.440 + 432.0/(T + 100.0) \qquad (T > 400\,°C)$$

5.1 Pre-buckling

The reduction of the free thermal expansion due to the force it causes in the restraint spring is $\delta_T = \alpha(T-20)l/(1+k_{ET}/\rho)$. The column is loaded (Figure 10(b)) at its top with a constant axial force P, which can be expressed as a proportion μ of the elastic buckling load $\pi^2 EI/l^2$. This causes an extra reduction of the free thermal expansion given by $\delta_P = P/(K + EAk_{ET}/l)$. This gives a total axial deflection (where δ is positive downwards) of Equation 14.

$$\begin{aligned}\delta &= (-\alpha(T-20)EAk_{ET}/K)/(1+EAk_{ET}/Kl) + P/(K+EAk_{ET}/l) \\ &= (-\alpha(T-20)k_{ET}l + Pl/EA)/(Kl/EA + k_{ET})\end{aligned} \qquad (14)$$

In dimensionless terms this can be expressed as $\overline{\delta} = (\overline{\mu}/k_{ET} - \alpha(T-20))/(1+\rho/k_{ET})$. As the steel temperature rises from 20°C to T°C the force F carried by the column is given by Equation 15.

$$F = P - K\delta \qquad (15)$$

If ϕ is the internal force ratio $F/(\pi^2 EI/l^2)$ then $\phi = \mu - \bar{\rho}\bar{\delta}$ and the column buckles elastically when $\phi = k_{ET}$.

5.1 Elastically post-buckled

After elastic buckling commences, post-buckling deflection hardly causes any change in the column force from the elastic buckling load, although this reduces with the elastic modulus reduction factor $k_{ET.}$

The basic equilibrium of Equation (15) always applies, so in dimensionless terms the normalised axial deflection is given by $\bar{\delta} = (\mu - k_{ET})/\bar{\rho}$.

It is worth examining the amplitude of the lateral deflection which corresponds to this axial shortening of the column. Assuming that the elastic buckle shape is a single half-sine wave, the first-order relationship between the normalised axial and lateral deflections shown in Figure 10(c) is $\bar{\delta}(1+\rho/k_{ET}) = \bar{\Delta}^2\pi^2/2 - \alpha(T-20) + \bar{\mu}/k_{ET}$.

5.2 Plastic post-buckling

Although the transition from elasticity to a plastic hinge mechanism requires too much detailed information about the cross-sectional properties of the column to be worth studying in detail, it is possible to look simply at the behaviour of the fully-plastic mechanism. It is assumed that the plastic moment capacity of the cross-section changes only with the yield strength reduction factor k_{yT}, shown in Figure 11(b), which is a reasonable assumption for slender columns but over-estimates moment capacity somewhat for stocky columns. The fully-plastic mechanism includes a single plastic hinge at the column's mid-height, as shown in Figure 10(d). Equilibrium now gives $P - K\delta = M_p k_{yT}/\Delta$. In dimensionless terms this is equivalent to $\mu - \bar{\rho}\bar{\delta} = \gamma k_{yT}/\bar{\Delta}$ where $\gamma = M_p/(\pi^2 EI/l)$.

The relationship between the axial column-top deflection and the mid-span deflection is approximately $\bar{\delta} = (\bar{\mu}/k_{ET} - \alpha(T-20) + 2\bar{\Delta}^2)/(1+\rho/k_{ET})$. In terms of the normalised lateral displacements this produces a cubic equation shown in Equation 16.

$$\bar{\Delta}^3 - \frac{\bar{\Delta}}{2}\left(\frac{\bar{\mu}}{\rho} + \alpha(T-20)\right) + \frac{\gamma k_{yT}}{2\bar{\rho}}(1+\rho/k_{ET}) = 0 \qquad (16)$$

This equation produces either one or three real roots for $\bar{\Delta}$ at any temperature, depending on the values of the coefficients in Equation (16). The single root is invalid, since it is negative, and therefore the plastic moments are in the wrong direction. The other pair of roots, when they exist, are valid and represent, respectively:

- Very small lateral deflection, so the column force is increased by its restrained negative deflection caused by thermal expansion. This is just equilibrated by the plastic moment, but is unstable if any positive increment of displacement occurs.

- Large lateral deflection, so that the column force is decreased by restrained positive deflection to the extent that the plastic moment can create equilibrium. This is a stable equilibrium state.

It can be seen from Figure 12, which plots the lateral displacement (or buckling amplitude) of the column, that the plastic mechanism phase produces a curve in which a destabilization occurs shortly after elastic buckling occurs, which is re-stabilized at higher amplitude. When translated to the equivalent axial displacement of the column top, shown in Figure 13, the effect is seen to become much more cuspid, and very similar to Figure 9, with the unstable plastic curve becoming almost tangential to the pre-buckled curve at the buckling temperature.

6 CONCLUSIONS

The behaviour of axially-restrained steel columns subject to heating has been explained in detail and this explanation has been validated against a non-linear finite element analysis using the Vulcan software.

By reducing the temperature of buckled columns, the snap-back behaviour of columns can be observed. This shows the ranges of the two stable solutions.

Whilst an isolated column has been modelled with a spring element providing axial restraint, this work is equally applicable to the case of a column as part of a frame, whereby the axial restraint is provided by beams framing in to the column. In these analytical models columns are shown to “hang” from the restraining spring after buckling. In a real building fire, a column would similarly exhibit unstable buckling behaviour before reaching a limit to its axial deflection by transferring load onto adjacent structure and “hanging” from its beams, providing that there is an alternative load path, along the beams and down the surrounding columns. However, in a fire scenario, these surrounding columns may also be hot, and may be just about to buckle. There is therefore the real possibility of a progressive collapse scenario, whereby a buckling column sheds its load through its beams onto the surrounding columns, which in turn then begin to buckle, shedding their load and that of the first column onto even more surrounding structure. The load-shedding is particularly likely to initiate buckling in the surrounding columns since it is dynamic.

An understanding of this change in load path, and the role that axial restraint plays in supporting the column after buckling, are extremely important in the design of steel frames. Often designs are optimised such that no one part of the structure is particularly weaker than another, and so when something fails it is likely that the surrounding structure is also close to failure. It has been shown that column buckling represents an extreme failure, where columns dynamically pass through an unstable region before restabilising through support from their axial restraint where available.

Since it has been shown that column buckling can lead to a hard failure which is sudden and can initiate progressive collapse, it is therefore suggested that steel frames are designed for robustness, with alternative load-paths provided which can accept the dynamic loads caused by column buckling. In particular, the effects of the spread of failure in fire from an origin should be considered.

REFERENCES

[1] Newman G.M, Robinson J.T & Bailey C G. (2006). "Fire Safe Design: A new Approach to Multi-storey Steel-framed Buildings (2nd Edition) SCI Publication P288", The Steel Construction Institute (SCI).

[2] Ali, F. A., Simms I., O'Connor D. (1997). "Effect of axial restraint on steel columns behaviour during fire", Proc. 5th Int. Fire Safety Conf., Melbourne, Australia.

[3] Rodrigues, J. P. C., Neves, I. C., Valente, J. C. (2000). "Experimental research on the critical temperature of compressed steel elements with restrained thermal elongation", Fire Safety J., 35 (2), pp77-98.

[4] Tan, K-H., Toh, W-S., Huang, Z-F. (2007). "Structural responses of restrained steel columns at elevated temperatures. Part 1: Experiments", Engineering Structures, 29 (8), pp1641-1652.

[5] Shepherd, P.G., Burgess, I.W., Plank, R.J. and O'Connor, D.J. (1997). "The Performance in Fire of Restrained Steel Columns in Multi-Storey Construction". Proc. 4th Kerensky Int. Conf., Hong Kong, pp333-342.

[6] Franssen, J-M. (2000). "Failure temperature of a system comprising a restrained column submitted to fire", Fire Safety J., 34 (2), pp191-207.

[7] Huang, Z-F., Tan, K-H. (2007). "Structural responses of restrained steel columns at elevated temperatures. Part 2: FE simulation with focus on experimental secondary effects", Engineering Structures, 29 (9), pp2036-2047.

[8] Wang, Y. C. and Moore, D. B. (1994). "Effect of thermal restraint on column behaviour in a frame", Proc. 4th Int. Symp. On Fire Safety Science, T. Kashiwagi, ed., Ottawa, pp1055-1066.

[9] Shepherd, P. G. (1999). "The Performance in Fire of Restrained Columns in Steel-Framed Construction", PhD Thesis, University of Sheffield, UK.

[10] Wong, M.B. (2005). "Modelling of axial restraints for limiting temperature calculation of steel members in fire", J. Constr. Steel Res. 61 (5), pp675-687.

[11] Bailey, C. G., Newman, G. M. (1996). "The behaviour of steel columns in fire", Steel Construction Institute Document RT524.

[12] Wang, Y. C. (2004). "Postbuckling Behavior of Axially Restrained and Axially Loaded Steel Columns under Fire Conditions", J. Struct. Eng. **130**(3), pp371-380.

Figure Captions

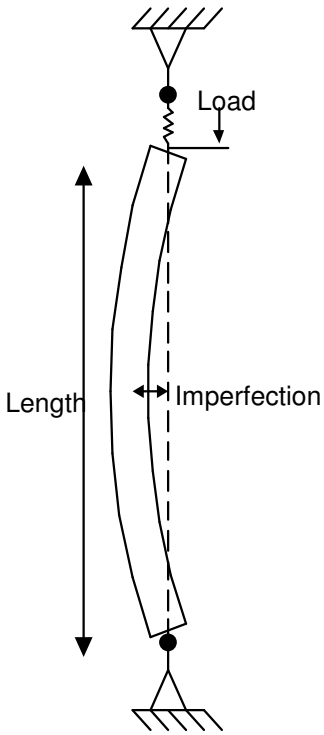

Figure 1 Analytical model

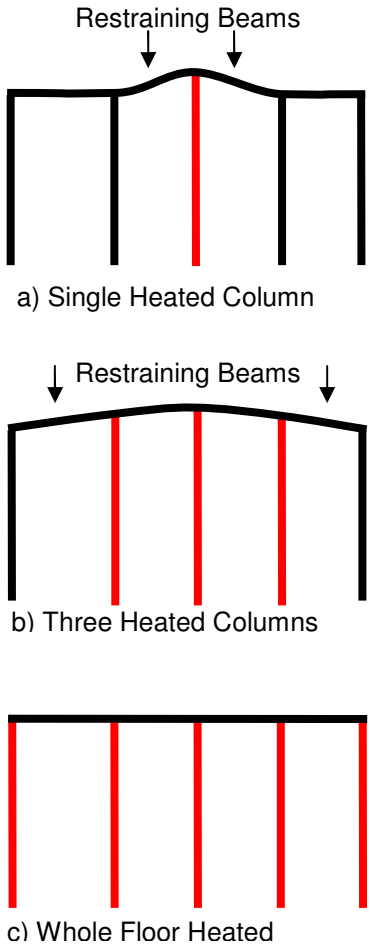

Figure 2 Single floor heating

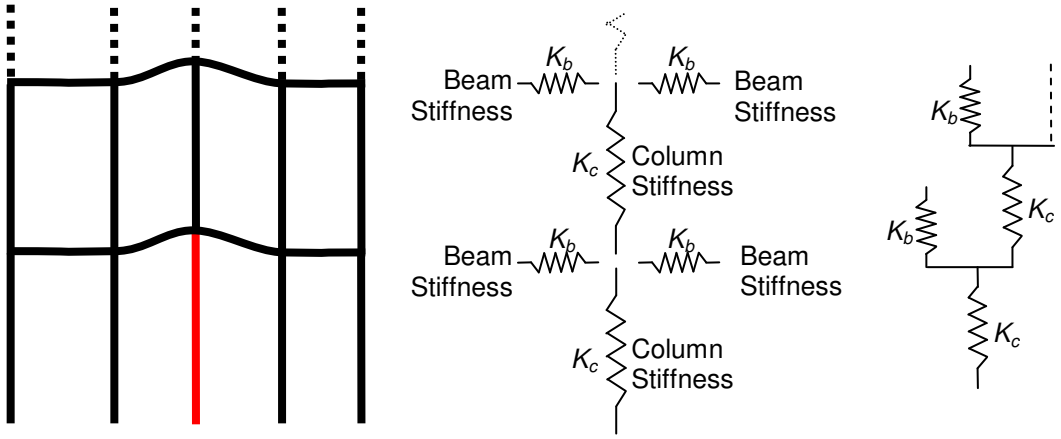

Figure 3 Multiple floor heating scenario, with equivalent- and combined-spring representation

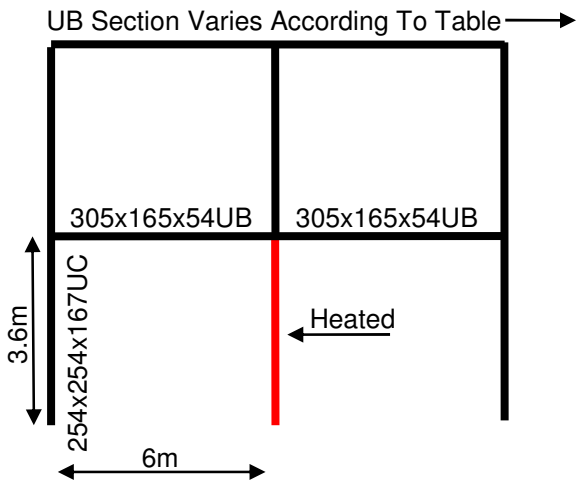

Top Beam Section	Restraint Ratio
305x127x48 UB	0.004
457x152x60UB	0.007
533x210x122 UB	0.017
610x305x179 UB	0.031
762x267x173 UB	0.041
762x267x197 UB	0.047
838x292x194 UB	0.055
914x305x201 UB	0.064
914x305x224 UB	0.073
914x305x253 UB	0.084
914x305x289 UB	0.097
914x419x388 UB	0.138

Figure 4 Heating scenario of chosen restraint values

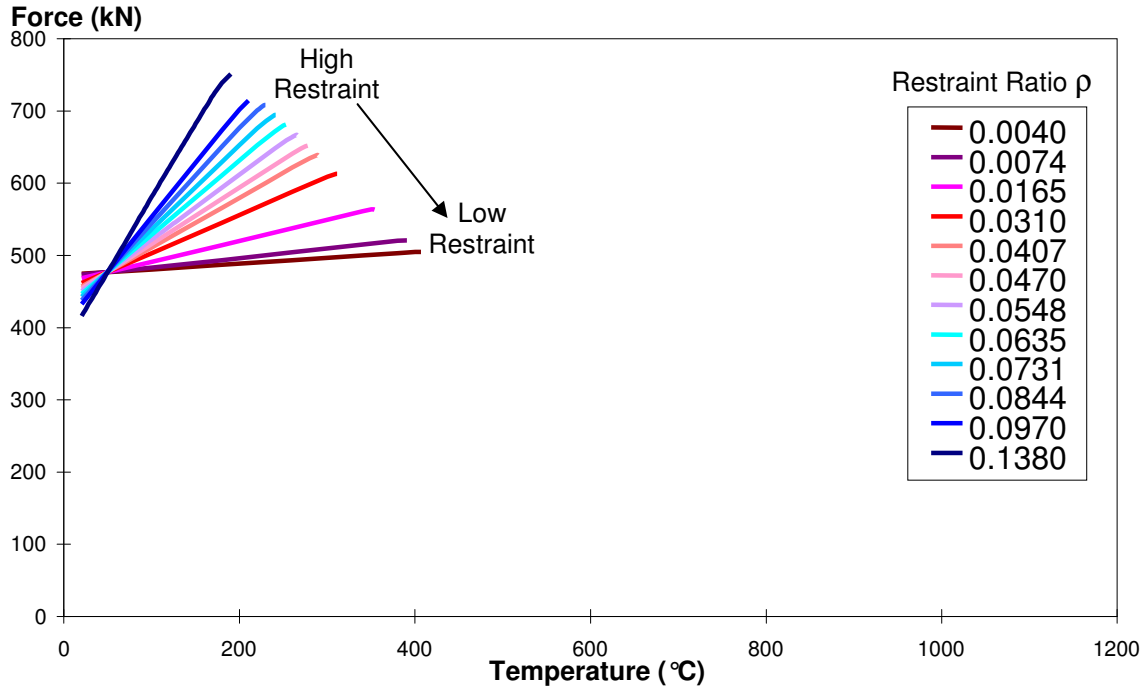

Figure 5 Force vs Temperature during “loading” phase

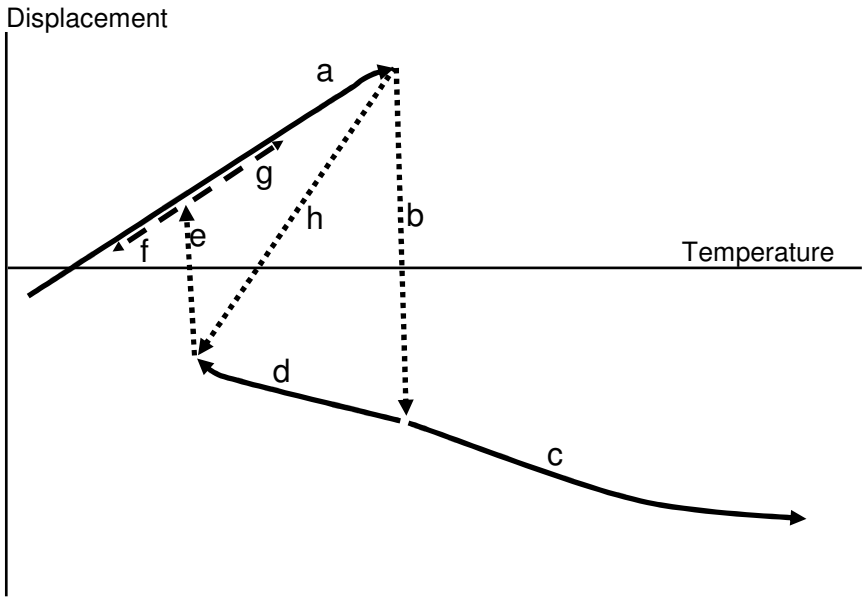

Figure 6 Schematic of column behaviour

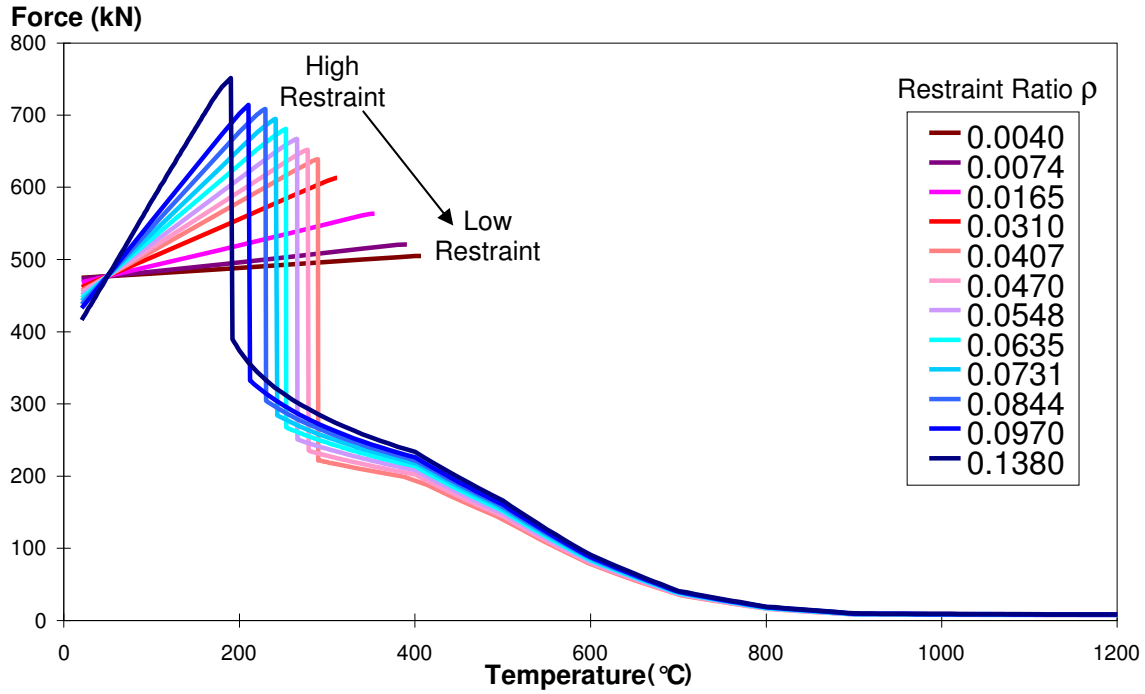

Figure 7 Force vs Temperature curves beyond “snap-through” phase

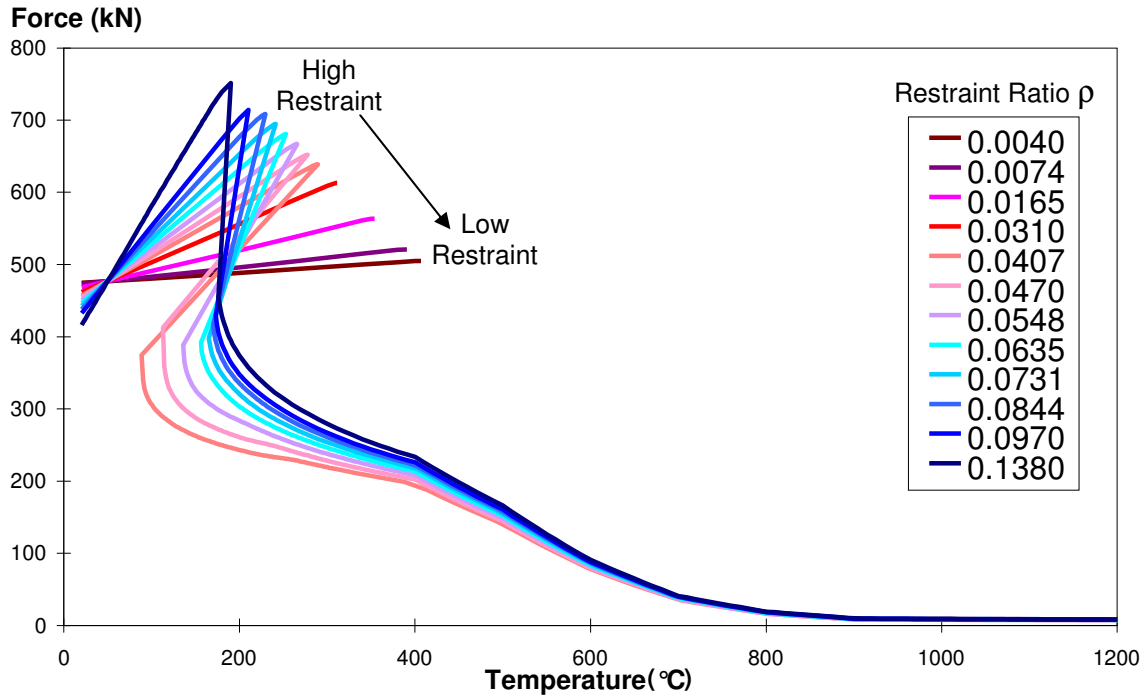

Figure 8 Full Force vs Temperature curves exhibiting “snap-back”

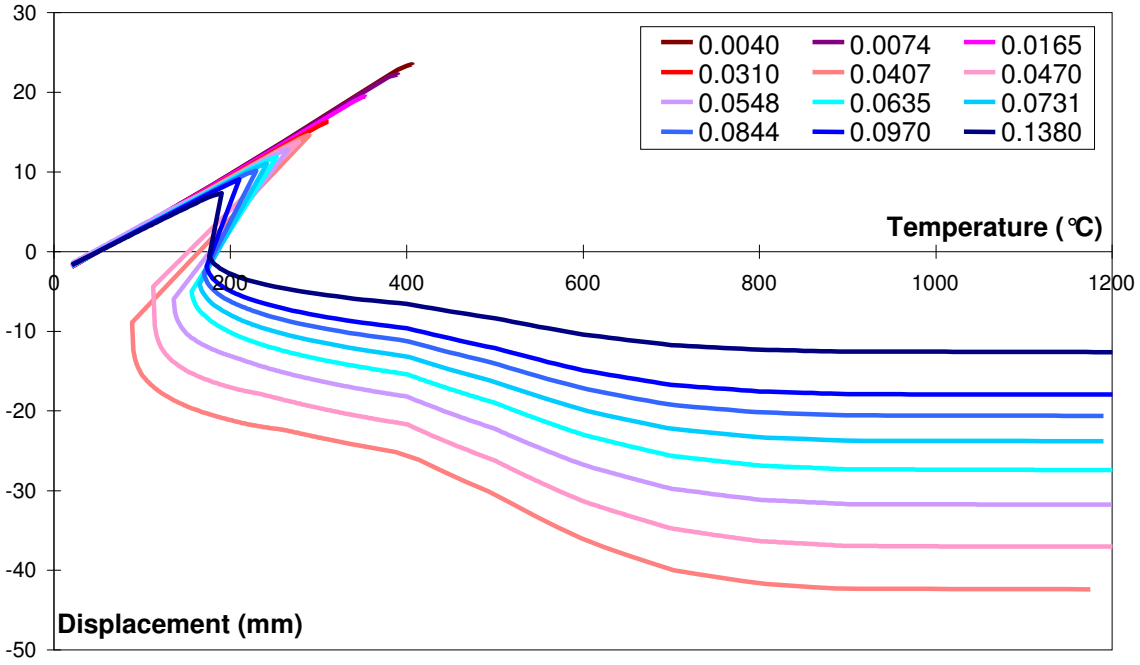

Figure 9 Vertical displacement of top of column

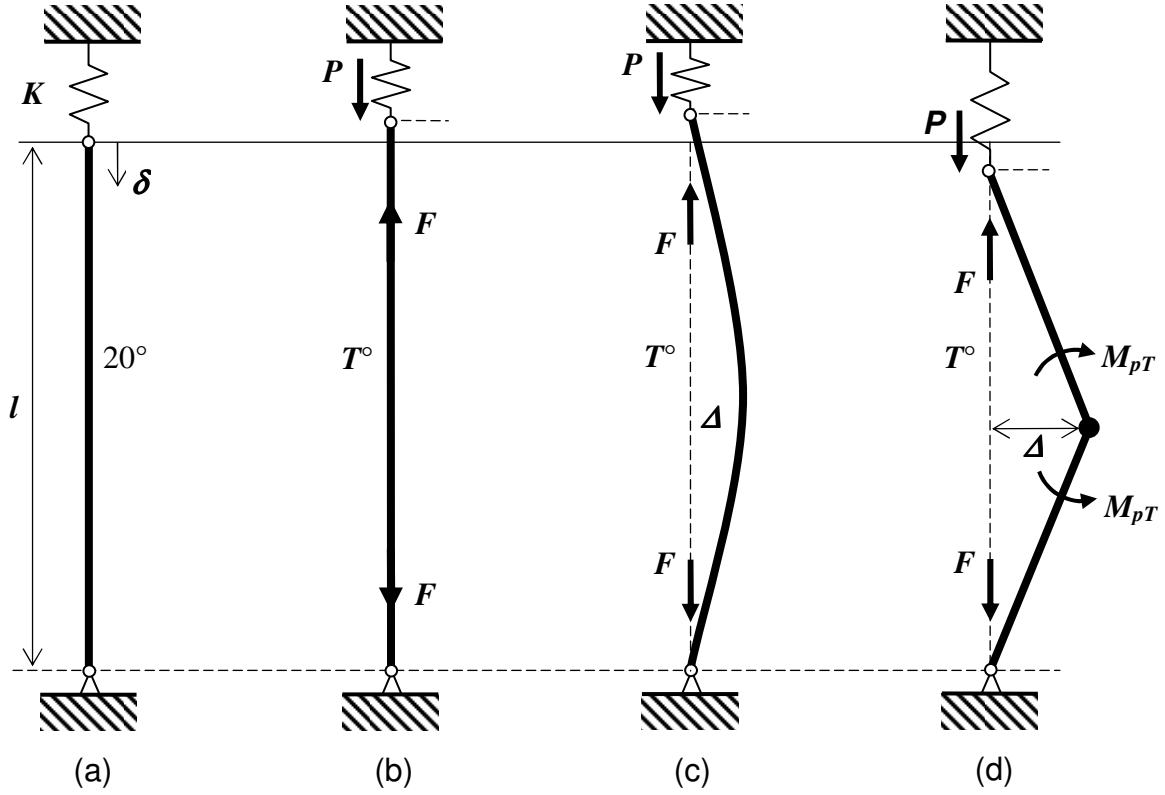

Figure 10 Simplified restrained column representations: (a) before loading or heating, (b) pre-buckling, (c) elastic buckling, (d) plastic buckling

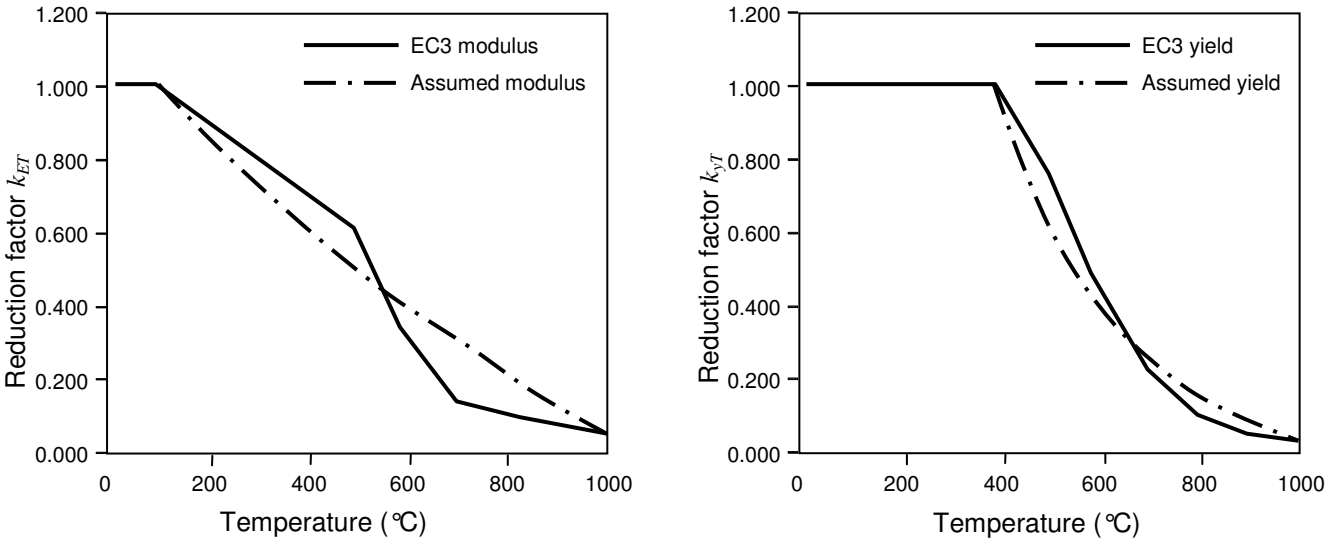

a) Elastic Modulus Degradation

b) Yield Strength Degradation

Figure 11 Assumed degradation of material properties with temperature

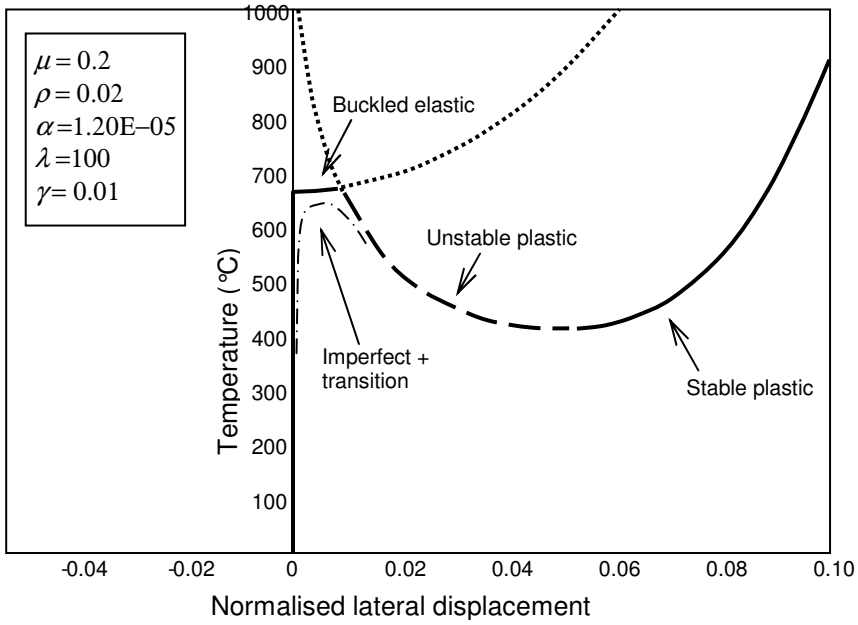

Figure 12 Lateral displacements of column mid-span

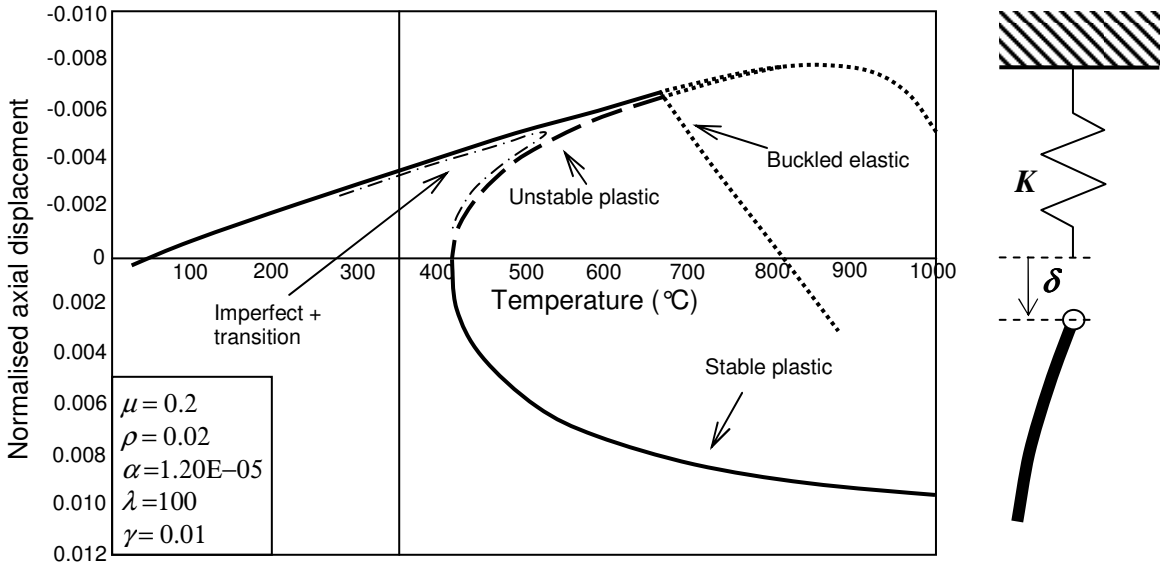

Figure 13 Axial displacements of column top